Supplementary Information

Iron phosphate mediated magnetite synthesis: a bioinspired approach

Giulia Mirabello‡*, Matthew GoodSmith‡, Paul H. H. Bomans, Linus Stegbauer, Derk Joester and Gijsbertus de With *

‡These authors contributed equally to this work.

*G. Mirabello (giulia.mirabello@gmail.com); G. de With (g.dewith@tue.nl).

Materials and methods

1. Magnetite synthesis

All reactions were carried out by using an automated titration system (Methrom Applikon) consisting of two 20 mL Dosino dosing units, a glass pH microelectrode and a magnetic stirring plate, all connected to two 901 Titrando titration units controlled by the TIAMO 2.2 software. All the solutions were prepared with Milli-Q water degassed with N_2 for at least 30 min prior to use. Also, the reaction solution was constantly flushed during the synthesis with wet argon gas. NaOH, H_3PO_4 and $FeCl_2 \cdot 4H_2O$ were purchased from Sigma-Aldrich, while $FeCl_3 \cdot 6H_2O$ were purchased from Merck and used as received. All the syntheses were performed at room temperature in 35 mL of total volume inside a 50 mL double-walled glass vessel. The overall synthetic set-up was placed inside a glovebox in an oxygen-free environment. Magnetite samples were "aged" in airtight, oxygen-free vials with a septum that allowed for sampling.

Stepwise reaction. The pH of a solution containing $FeCl_3$ (0.02 M) and H_3PO_4 (0.03 M) was increased to 3 by addition of NaOH 0.5 M and a light-yellow precipitate was formed. The light-yellow precipitate was isolated, washed with distilled water several times, and resuspended in a solution contacting $FeCl_2$ (0.01 M) at pH 3 (solution 2). The pH of this solution was then increased to 12 by the addition of NaOH 0.5 M.

Co-precipitation. The pH of a solution containing $FeCl_3$ (0.02 M), $FeCl_2$ (0.01 M) and H_3PO_4 (0.03 M) was increased to 12 by addition of NaOH 0.5 M.

Control. For purposes of comparison, magnetite was synthesized through simple coprecipitation in the absence of H_3PO_4 using the same titration program. Namely, the pH of a solution containing $FeCl_3$ and $FeCl_2$ in stochiometric ratio of 2:1 was increased to 12 by addition of NaOH 0.5 M. One magnetite sample prepared in this way was later oxidized by bubbling O_2 gas for 8 hours, and the resulting brown solid was used as the maghemite standard.

2. Amorphous ferrous and ferric phosphate

For comparison, amorphous ferrous and ferric phosphates were synthesized separately by increasing the

pH of a solution containing H_3PO_4 (0.03 M) and either $FeCl_3$ (0.03 M) or $FeCl_2$ (0.03 M) to 12 by addition of NaOH 0.5 M. The reaction was carried out by using the same experimental setup described for magnetite synthesis (see above).

3. Transmission electron microscopy

For conventional dry TEM, 200 mesh Cu grids with continuous carbon films (Agar Scientific) were used. Sample preparation was performed by applying 50 µL of solution onto the TEM grid and drying by air. For cryo-TEM, samples were prepared on 200 mesh Cu grids with Quantifoil R 2/2 holey carbon films (Quantifoil Micro Tools GmbH). The cryogenic samples were prepared by employing an automated vitrification robot (FEI Vitrobot™ Mark III) to plunge each sample in liquid ethane in preparation for cryo-TEM.[1] All TEM grids were surface plasma treated for 40 seconds using a Cressington 208 carbon coater prior to use. Conventional dry samples were analyzed on a FEI Technai 20 (type Sphera) operated at 200 kV, equipped with a LaB_6 filament and a 1k × 1k Gatan CCD camera. Cryogenic samples were analyzed on the TU/e cryoTITAN (FEI, www.cryotem.nl) operated at 300 kV, equipped with a field emission gun (FEG), a postcolumn Gatan Energy Filter (GIF) and a post-GIF 2k × 2k Gatan CCD camera. Gatan DigitalMicrograph™ by Gatan Inc. (including DiffTools), and MATLAB by MathWorks were used for TEM image and SAED pattern analysis.

4. Image and electron diffraction analysis and processing

For display reasons, enlargements of the cryo-TEM images were bilinearly interpolated with Adobe Photoshop™, while the image analysis was performed on the original non-processed files.
The low dose selected area electron diffraction (LD-SAED) patterns obtained were analyzed by radially averaging the intensity resulting in the so-called radial intensity profile. This analysis was performed with the use of a MATLAB script. The center of the ED pattern was determined manually by selecting 4 points on one of the concentric circles. The center was then used to produce a profile plot of normalized integrated intensities as a function of the distance of the diffraction rings from the center. It is important to note that the beam-stopper was not integrated as it was removed by applying a mask. This procedure allowed for the determination of the *d*-spacing of each reflection.

5. Crystal size measurements

Crystal size distributions were determined by manually measuring the long and short axes of more than 100 individual crystals per sample in TEM images using a MATLAB script. The average of long and short axis for each crystal was taken as the crystal size. Crystal sizes are reported as mean ± standard deviation of the mean.

6. Raman Spectroscopy

Raman spectroscopy was performed on a Jobin-Yvon Labram spectrometer equipped with a HeNe laser (excitation wavelength 632.81 nm), a holographic grating (600 grooves/mm), an ultra-long working distance objective (Olympus, magnification 100 ×, numerical aperture 0.8) and a CCD camera.
Slides were prepared for Raman spectroscopy in an oxygen-free environment using custom glass slides that allow for the measurement of particles in solution (see Fig. S1). An epoxy seal around the solution ensured minimal oxygen in the measured solution. This immersion set-up was necessary given the

oxygen-sensitive nature of products containing Fe^{2+}. A standard Filter function in the Labspec software was applied to curves with prohibitively large signal-to-noise ratios.

7. Powder X-ray Diffraction

PXRD data were collected at room temperature on a STOE-STADI-MP powder diffractometer equipped with an asymmetric curved Germanium monochromator (MoKα1 radiation, λ = 0.70930 Å) and one-dimensional silicon strip detector (MYTHEN2 1K from DECTRIS). The line-focused Mo X-ray tube was operated at 50 kV and 40 mA. Powder was packed in an 8 mm metallic mask and sandwiched between two layers of polyimide tape. The instrument was calibrated against a NIST Silicon standard (640d) prior to the measurement. Please note that the Mo radiation was used because of high background due to Fe-fluorescence when using Cu radiation. The PXRD of magnetite with different particle size was simulated based on the CIF filed derived from ref (American Mineralogist, Volume 85, pages 514–523, 2000) with the help of Crystalmaker CrystalDiffract(R) for Windows 6.5.0 (CrystalMaker Software Limited, Oxford, UK) and its implemented simulation of the Scherrer equation.

8. Micro-X-ray near edge structure (μXANES)

X-ray absorption spectro-microscopy at the iron K-edge was performed at the GSECARS X-ray microprobe beamline (13-ID-E) at the Advanced Photon Source (APS), Argonne National Laboratory (Lemont, IL USA).[2] Powdered reference samples were spread uniformly on double-sided tape. Using a beam focused to 1 × 1 μm^2, X-ray fluorescence (XRF) maps were recorded to determine regions of interest (ROI) for subsequent μXANES. XANES spectra were collected in fluorescence mode using a four-element, silicon-drift-diode detector array (Vortex-ME4, Hitachi High-Technologies Science America, Inc.), with pulse-processing provided by an Xspress 3 digital X-ray processor system (Quantum Detectors). The incident beam energy was scanned in 6 eV steps from 7012 to 7102 eV, in 0.1 eV steps from 7102 to 7132 eV, and in 1.5 eV steps from 7132 to 7740 eV, with a dwell time of 0.5 s. All spectra were recorded under a helium atmosphere. Under these conditions, single scans resulted in spectra of sufficient quality for analysis. Spectra were calibrated to the inflection point of zero-valent Fe foil (E_0 = 7110.75 eV),[3] and were normalized to the incident beam intensity (I_0) measured in a helium-filled, 200 mm-long ion chamber just upstream of the KB mirror optics. All XANES data were corrected for detector dead time, self-absorption and normalized with Athena.[4] Pre-edge features were isolated by fitting, and then subtracting, an inverse tangent (arctan) function to the main edge. The pre-edge, i.e. the residual from the first step, was then fit with three Gaussian components, using MATLAB (Mathworks, Natick, MA). Gaussian component 2 and 3 represent 1s→3d transitions and were fit with the same full width at half maximum (FWHM). Gaussian component 1 does not arise from a 1s→3d transitions was fit with an independent FWHM.[5]

As an example of how we calculated the centroid position[5] we report the case of Fe^{3+}/P 1:1, pH = 6 sample. The intensities of all Gaussian components of the Fe^{3+}/P 1:1, pH = 6 sample are summed up:

$$0.060 + 0.042 = 0.102 \quad Eq.(1)$$

This is the sum of all intensities used for intensity weighing. Then we add the intensity-weighted average of the components' positions to obtain the centroid (center of mass of the area below the peak):

$$\frac{0.06}{0.102} \cdot 7112.75\ eV + \frac{0.042}{0.102} \cdot 7113.75\ eV\ =\ 7113.16\ eV \qquad Eq.(2)$$

This value and the sum of the intensities (Eq. (1)) is then compared to Figure 4 in Wilke et al., Am. Mineral. 86 714-730.[5] Wilke et al. have determined that there is a correlation between the centroid, integrated intensity of the pre-edge peaks, and the oxidation state/coordination environment of the iron atom. Based on this comparison, we estimate that an octahedral coordination environment around the Fe^{3+} is present in the Fe^{3+}/P 1:1, pH = 6 sample.

Table S1. Spectral deconvolution of pre-edge region of Fe K-edge XANES spectra using three gaussian components.

Sample	Component G1			Component G2			Component G3			Sum of squared residuals
	mean (eV)	FWHM (eV)	area fraction	mean (eV)	FWHM (eV)	area fraction	mean (eV)	FWHM (eV)	area fraction	
(Fe^{3+} Fe^{2+})/P 1:1, pH = 6	7111.13	1.71	0.012	7112.71	1.72	0.041	7113.93	1.72	0.031	$4.0*10^{-6}$
Fe^{3+}/P 1:1, pH = 6	-	-	-	7112.75	1.93	0.060	7113.75	1.93	0.042	$3.0*10^{-6}$

Table S2. Comparison of the pre-edge centroid positions to estimate the Fe^{2+} content assuming a linear shift to lower energies by 1.5 eV going from Fe^{3+} to Fe^{2+} (see ref. 5)

Sample	Centroid	Fe^{2+} content
(Fe^{3+} Fe^{2+})/P 1:1, pH = 6	7112.93	15%
Fe^{3+}/P 1:1, pH = 6	7113.16	0%

[a)] intensity-weighted average of the components' positions

Table S3. Comparison of XANES data of the $Fe^{2+}Fe^{3+}$ co-precipitate and the Fe^{3+} precipitate at pH=6.

Sample	Pre-edge	E_0[a]	A[b]	B[b]	C[b]	D[b]
$Fe^{2+}Fe^{3+}$ (Fe/P 1:1)	7111.13 7112.71 7113.93	7122.7	7130.4	7135.7	Not visible	7183.7
Fe^{3+} (Fe/P 1:1)	7112.75 7113.75	7122.5	7131.0	7136.6	7147.2	7188.92

[a)] Deduced from the maxima in the first derivative of the spectrum. [b)] Deduced from the minima in the second derivative of the spectrum (not shown).

Table S4. Comparison of the edge energy at normalized intensity = 0.5. Fe^{2+} content is estimated assuming a linear shift to lower energies according to according to Baumgartner et al., *Proc. Natl. Acad. Sci.,* 2013, and Fdez-Gubieda et al., *ACS Nano*, 2013.[6,7]

Sample	Energy at norm. I=0.5	Fe^{2+} content
magnetite reference	7121.1	33%
(Fe^{3+} Fe^{2+})/P 1:1, pH = 6	7122.7	10%
Fe^{3+}/P 1:1, pH = 6	7123.4	0%

Supplementary figures

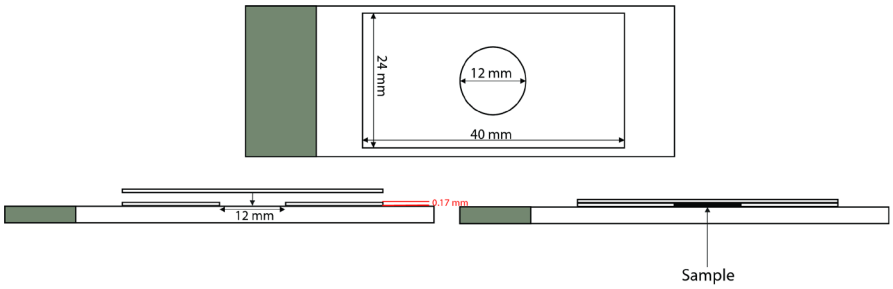

Fig. S1 Sample holder for Raman spectroscopy measurements. The sample is placed inside the small round cavity (12 mm wide and 0.17 mm thick) and subsequently sealed with epoxy to avoid oxidation.

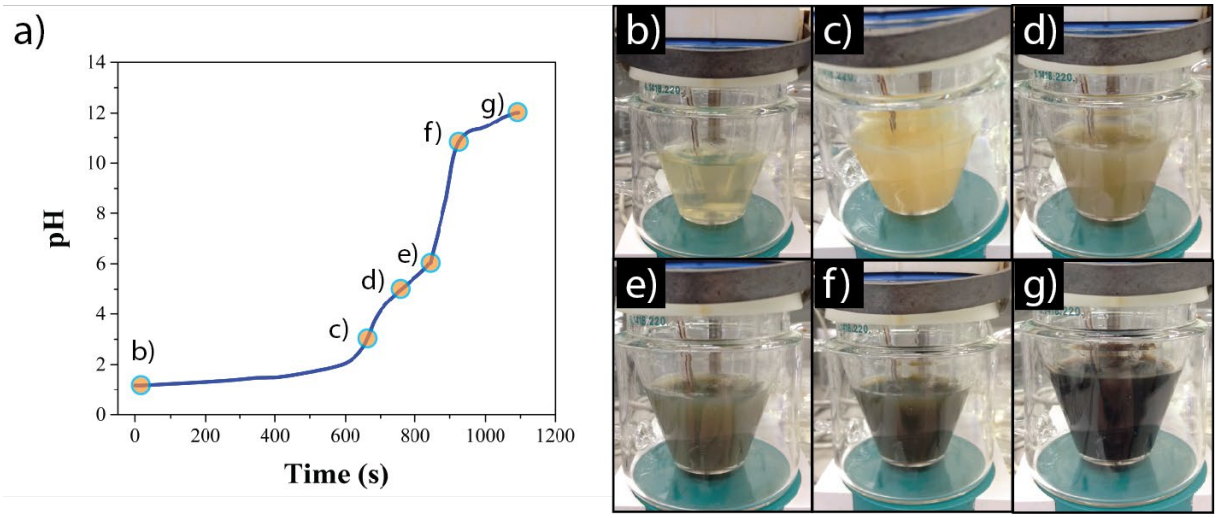

Fig. S2 Typical color changes and pH profile during synthesis. a) pH curve profile. b) pH 1.18 (initial); c) pH 3 (whitish-yellow product); d) pH 4.96; e) pH 6 (green product); f) pH 10.45; g) pH 12 (black product); g) Three separate precipitation events are reflected in the pH curve. Note: the sudden slope change at pH 6 occurred because we increased the addition rate between pH 6 and pH 12 in this reaction sequence.

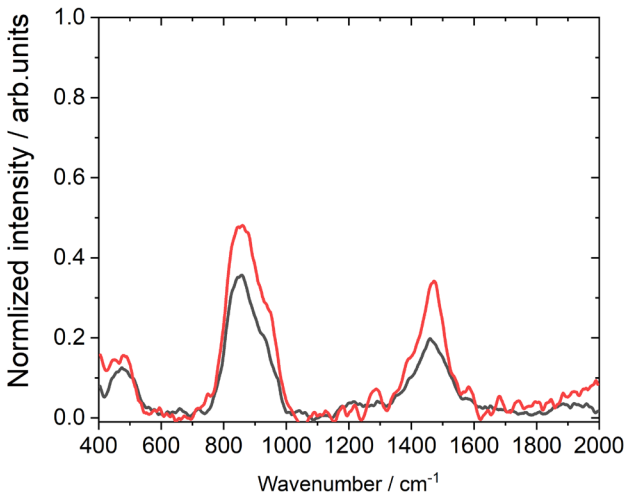

Fig. S3 Raman spectra of the iron phosphate obtained at pH 6 via stepwise (red) and co-precipitation (black) reactions.

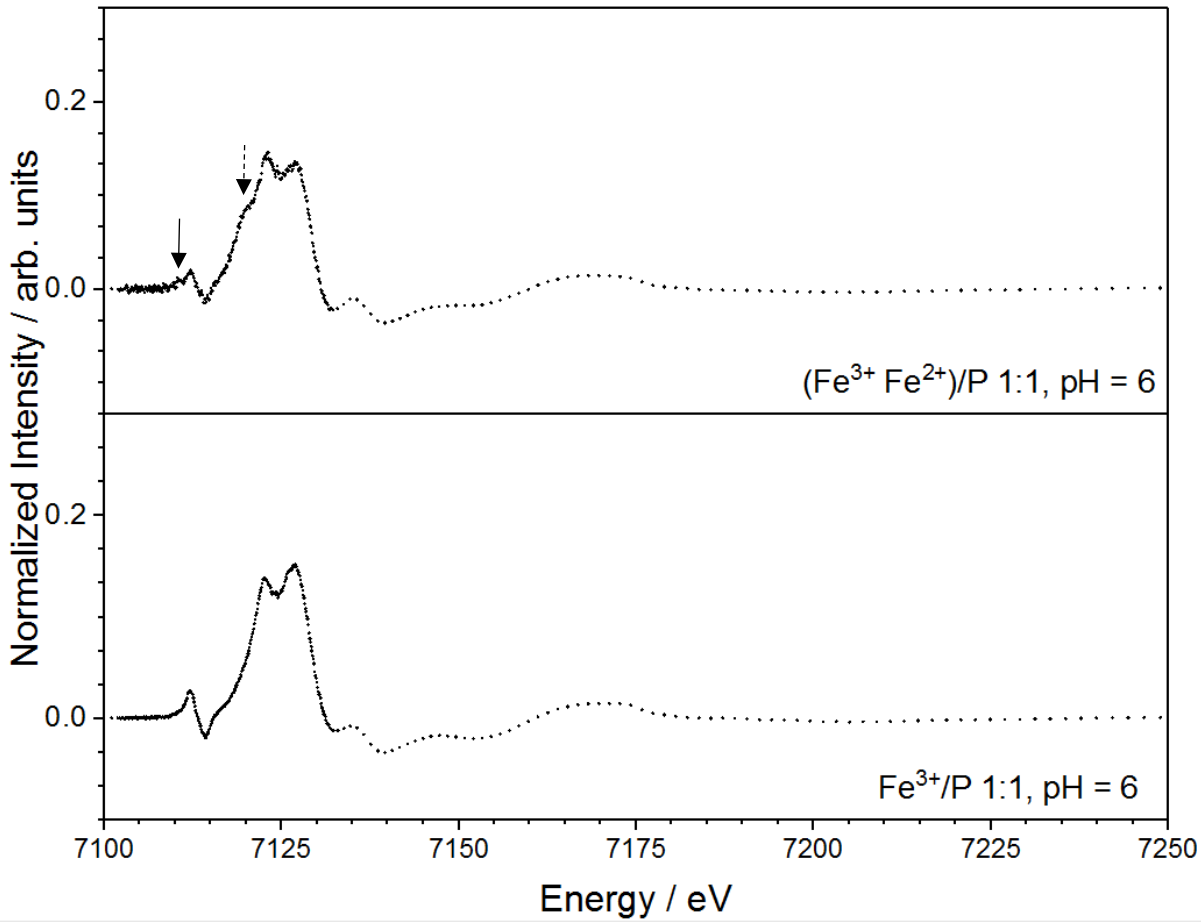

Figure S4 1st derivative of the X-ray absorption fine structure (XAFS) spectra of the $Fe^{2+}Fe^{3+}$ co-precipitated phosphate and the Fe^{3+} phosphate. The black arrows point to features indicating the presence of Fe^{2+}. The solid arrow shows the presence of an additional shoulder at lower energies in the pre-edge corresponding to an inflection point in the spectrum. The dashed arrow shows a shoulder, which corresponds to 7120.3 eV indicating the slightly lower E_0 energy of the Fe^{2+} ions in the sample.

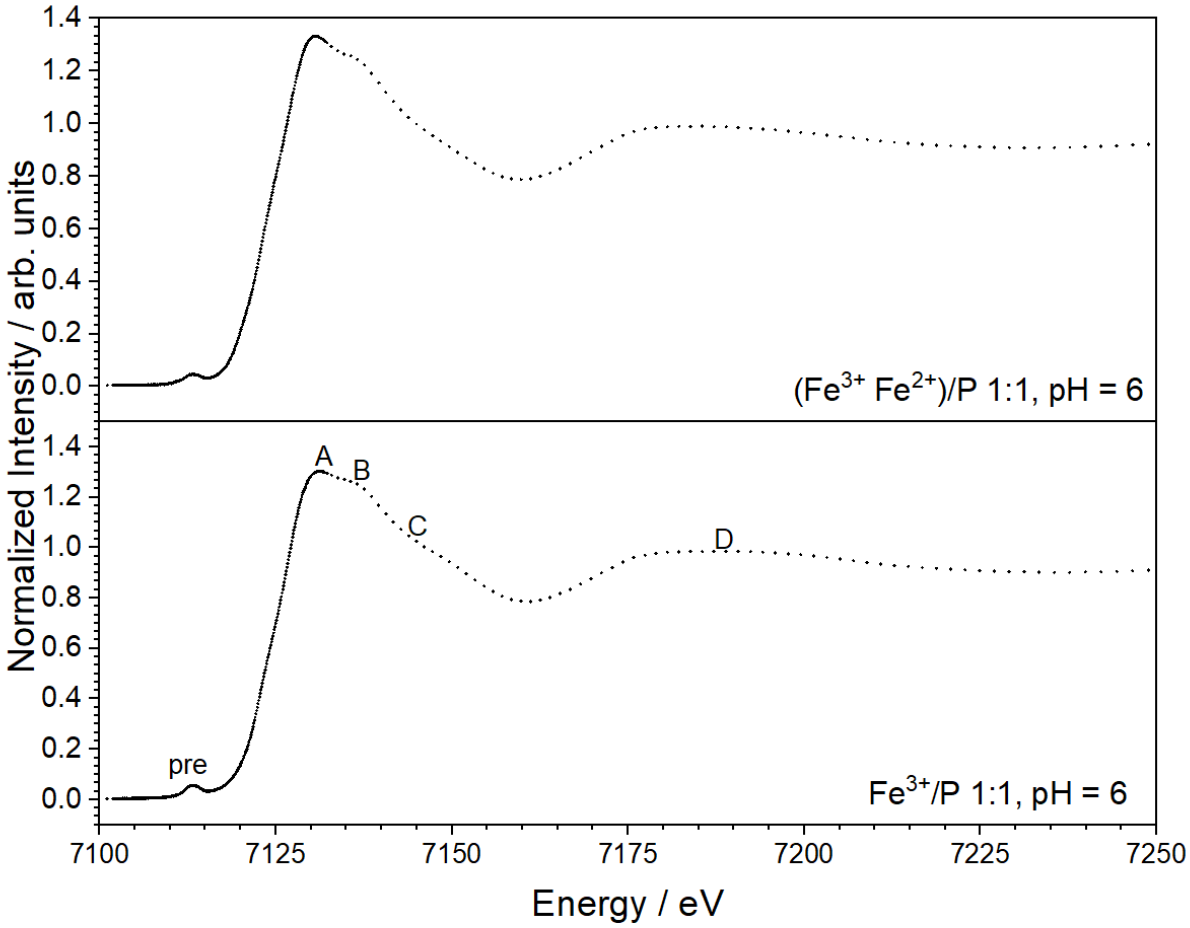

Figure S5 XAFS spectra of the $Fe^{2+}Fe^{3+}$ co-precipitated phosphate and the Fe^{3+} phosphate showing the positions chosen for comparison of the two spectra.

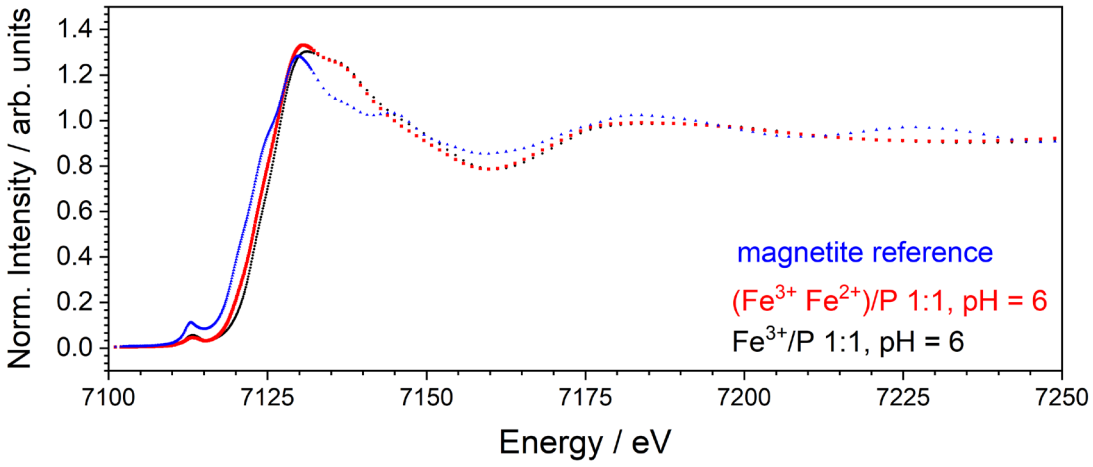

Figure S6 Direct comparison of the XAFS spectra of the the magnetite reference (blue), the Fe^{2+} Fe^{3+} co-precipitated phosphate (red) and the Fe^{3+} phosphate (black) indicating a clear shift to lower energies with increasing amounts of Fe^{2+} in the sample.

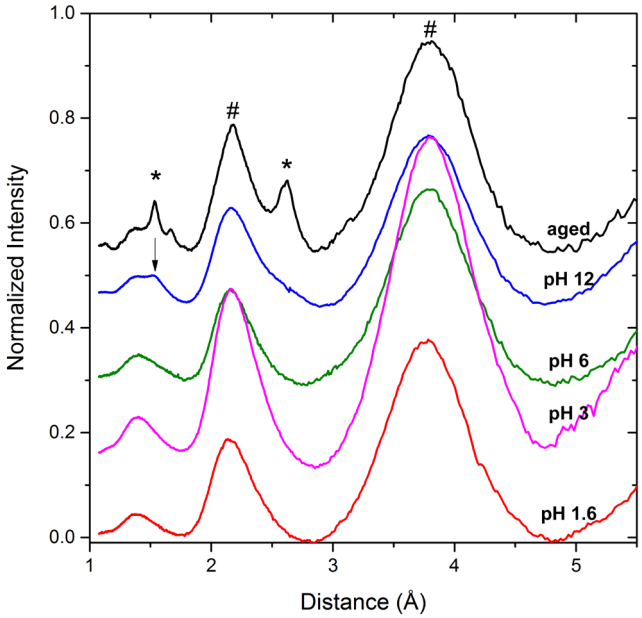

Fig. S7 Radial intensity profile of the of the low-dose cryogenic electron diffraction (LD-cryo-ED) patterns of samples at pH 1.6 (red), pH 3 (pink), pH 6 (green), pH 12 (blue). The black curve is the ED of the 5 weeks aged product showing the typical reflections for magnetite mineral phase indicated by the * symbol at ~ 1.5 Å (440) and 2.55 Å (311). The # symbol indicates the reflections corresponding to the signal of the vitrified water layer at ~ 2.16 and 3.80 Å. Dose rate ~ 3.76 $e^{-}\cdot Å^{(-2)}\cdot s^{(-1)}$.

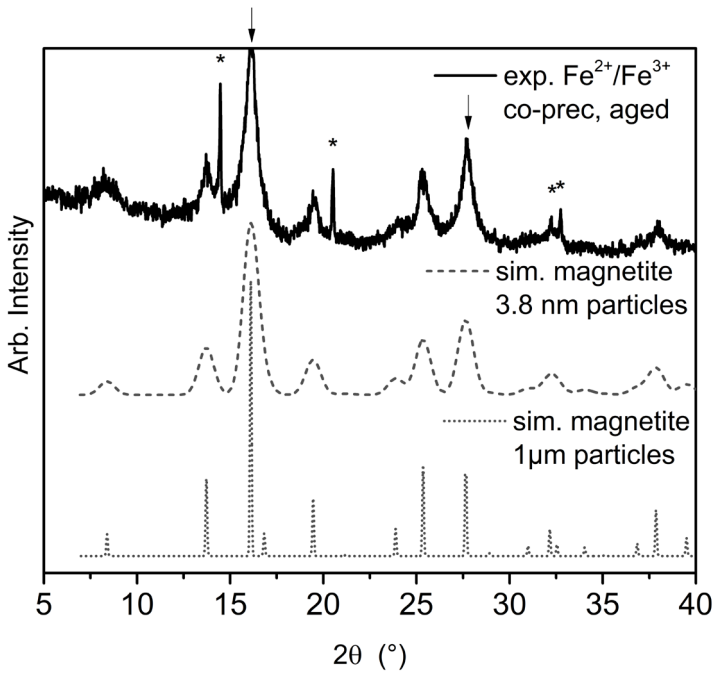

Fig. S8 Powder x-ray diffraction pattern of the aged Fe^{2+}/Fe^{3+} precipitate (end product obtained at pH 12) in presence of phosphate (solid line top pattern), magnetite from ref [8] simulated with 3.8nm particle size (dashed line mid pattern), and magnetite from ref [8] simulated with 1 µm particle size (dotted line bottom pattern). The asterisks indicate the reflections of NaCl, which is present as an impurity in the experimental pattern. The arrows indicate the characteristic reflections of magnetite at 16.1° 2θ and 27.7° 2θ corresponding to the crystallographic planes 440 and 311. The abbreviations exp, sim, co-prec and arb stand for experimental, simulated, coprecipitated and arbitrary, respectively.

References

1 M. R. Vos, P. H. H. Bomans, P. M. Frederik and N. A. J. M. Sommerdijk, *Ultramicroscopy*, 2008, **108**, 1478–1483.

2 S. R. Sutton, A. Lanzirotti, M. Newville, M. L. Rivers, P. Eng and L. Lefticariu, *J. Environ. Qual.*, 2017, **46**, 1158–1165.

3 S. Kraft, J. Stümpel, P. Becker and U. Kuetgens, *Rev. Sci. Instrum.*, 1996, **67**, 681–687.

4 B. Ravel and M. Newville, *J. Synchrotron Radiat.*, 2005, **12**, 537–541.

5 M. Wilke, F. Farges, P.-E. Petit, G. E. Brown Jr. and F. Martin, *Am. Mineral.*, 2001, **86**, 714–730.

6 J. Baumgartner, G. Morin, N. Menguy, T. P. Gonzalez, M. Widdrat, J. Cosmidis and D. Faivre, *Proc. Natl. Acad. Sci. U. S. A.*, 2013, **110**, 14883–14888.

7 M. L. Fdez-Gubieda, A. Muela, J. Alonso, A. García-Prieto, L. Olivi, R. Fernández-Pacheco and J. M. Barandiarán, *ACS Nano*, 2013, **7**, 3297–3305.

8 C. Haavik, S. Stølen, H. Fjellvåg, M. Hanfland and D. Häusermann, *Am. Mineral.*, 2000, **85**, 514–523.